DOI: 10.1002/htj.21428

WILEY

ORIGINAL ARTICLE

Heat transfer study of convective fin with temperature-dependent internal heat generation by hybrid block method

Mohammad Alkasassbeh[1] | **Zurni Omar**[1] | **Fateh Mebarek-Oudina**[2] | **Jawad Raza**[1,3] | **Ali Chamkha**[4,5]

[1]School of Quantitative Sciences, Universiti Utara Malaysia, Sintok, Malaysia

[2]Department of Physics, Faculty of Sciences, University of Skikda (University of 20 août 1955-Skikda), Skikda, Algeria

[3]Department of Mathematics and Statistics, Institute of Southern Punjab (ISP), Multan, Pakistan

[4]Department of Mechanical Engineering, Prince Mohammad Endowment for Nanoscience and Technology, Prince Mohammad Bin Fahd University, Al-Khobar, Saudi Arabia

[5]RAK Research and Innovation Center, American University of Ras Al Khaimah, Ras Al Khaimah, United Arab Emirates

Correspondence
Fateh M. Oudina, Department of Physics, Faculty of Sciences, University of Skikda, B.P 26 Road El-Hadaiek, Skikda 21000, Algeria.
Email: oudina2003@yahoo.fr; f.mebarek_oudina@univ-skikda.dz

Abstract

Purpose: In this study, an implicit one-step hybrid block method using two off-step points involving the presence of a third derivative for solving second-order boundary value problems are subjected to Dirichlet-mixed conditions.

Methodology: To derive this method, the approximate power series solution is interpolated at $\{x_n, x_{n+\frac{2}{5}}\}$ while its second and third derivatives are collocated at all points $\{x_n, x_{n+\frac{2}{5}}, x_{n+\frac{3}{5}}, x_{n+1}\}$ on the integrated interval of approximation.

Findings: The new derived method not only performs better compared with the existing methods when solving the same problems but also obtains better properties of the numerical method. Afterward, the proposed method is applied to solve the problem of a convective fin with temperature-dependent internal heat generation. The effects of various physical parameters on temperature distribution are also examined.

KEYWORDS

convective fin, heat transfer, hybrid block method, interpolation, thermal analysis

1 | INTRODUCTION

Typically, a fin is a fundamental mechanical body part that contributes mostly in raising the rate of heat transfer, as it is capable of expanding the area of heat transfer, which, in turn, results in a greater amount of heat being transferred (according to Kraus et al[1]). Furthermore,

fins are extensively used in the industry, for instance, in vehicles, airplanes, modern chips, and heavy machinery. Fins come in different shapes but the rectangular shape is the best-known. The reason behind this has to do with the usefulness of this design and its value in improving the manufacturing productivity. In considering the common fins problem, the thermal conductivity usually remains constant. However, if there is a significant temperature difference between the top and bottom of the fin, the temperature effect on the thermal conductivity must be taken into account. Also, it is logical to consider heat imitation generated by the electrical current. The efficiency of heat transfer and refrigeration for fully wet circular porous fins together with rectangular, triangular, and convex sections was examined analytically by Hatami and Ganji.[2,3] Ghasemi et al[4] examined the accuracy of semianalytical method of nonlinear temperature distribution in a longitudinal fin. In this study, temperature-dependent heat generation and thermal conductivity of the fin were analyzed by using the differential transformation method (DTM). Least square method (LSM), collocation method, and fourth-order Runge-Kutta method were used to examine the effects of heat transfer and temperature distribution on semispherical convective-radiative porous fins.[5] The results revealed that LSM had excellent agreement with the numerical method for the variations of different physical parameters raised in the problem under consideration.

Many methods have been used for predicting the behavior of a longitudinal fin with temperature-dependent internal heat generation and thermal conductivity. Among the authors of such research are Aziz and Bouaziz,[6] who proved that the result of the LSM is much simpler than the homotopy perturbation method (HPM), variational iteration method (VIM), or double series regular perturbation method. Razani and Ahmadi,[7] contrarily, identified an optimum circular fin design by investigating nonlinear temperature-dependent thermal conductivity in the presence of a heat source distribution. Ünal[8] performed research on the rectangular and longitudinal fins in the presence of temperature-dependent internal heat generation and a temperature-dependent heat transfer coefficient.

Ghadikolaei et al[9] analyzed the problem of an incompressible homogeneous second-grade fluid over a stretching sheet channel with HPM. The fluid flow problem of blood containing nanoparticles in a porous medium under the influence of the magnetic field was studied using Akbari-Ganji's collocation method.[10] Similarly, the problems of fluid flow between two parallel walls under the influence of various physical parameters were analyzed under the various fluid flow conditions.[11-13]

In the same vein, Shouman[14] conducted a similar study on both temperature-dependent thermal conductivity and internal heat generation. Following the same strategy, Kundu[15] and Domairry and Fazeli[16] continued the research on different fin shapes. The former solved a problem regarding thermal analysis and the optimization of longitudinal and pin fins of uniform thickness subject to fully wet, partially wet, and fully dry surface conditions, while the latter solved the nonlinear straight fin differential equation by the homotopy analysis method (HAM) to evaluate the temperature distribution and fin efficiency.

Ganji et al[17] used the HPM method to carry out a study on the temperature distribution for annular fins with temperature-dependent thermal conductivity. The effects of the temperature-dependent thermal conductivity of a moving fin considering the radiation losses have been studied by Aziz and Khani.[18] Bouaziz and Aziz[19] introduced a double optimal linearization method (DOLM) to get a simple and accurate solution for the temperature distribution in a straight rectangular convective-radiative fin with temperature-dependent thermal conductivity.

This study discusses the model for the distribution of heat across different types of fins, which is expressed as a boundary value problem (BVP). In most cases, this BVP fails to obtain an analytical solution. Thus, many scholars have made efforts to develop a numerical method for such BVPs,

such as finite difference methods, the Adomian decomposition method, and interpolation and collocation methods. Their interpolation approach has been widely used by authors, such as Kayode and Adeyeye,[20] Badmus,[21] and Kuboye and Omar[22] due to its simplicity in developing the block method and also the ease of writing its computer programs. Unfortunately, block methods cannot overcome the Dahlquist barrier, which stipulates that "the order of a k-step linear multistep block method cannot exceed $k + 1$ (k is odd) or $k + 2$ (k is even) for the method to be zero-stable. To tackle this weakness, hybrid block methods (HBMs) have been proposed by several authors. For example, Anake et al[23] examined HBMs involving one-step with two off-steps. Meanwhile, Adeyeye[24] derived a two-step HBM including two off-steps for solving second-order ordinary differential equations (ODEs) with the help of Chebyshev polynomials. However, the accuracy regarding error was not very efficient. Two years later, Omar and Abdelrahim[25] developed a one-step HBM with generalized three off-steps using interpolation and collocation for solving second-order initial-value problems (IVPs). Similarly, Abdelrahim and Omar[26] derived a one-step HBM with generalized two off-steps using interpolation and collocation for solving third-order IVPs. The following year, Omar and Abdelrahim[27] proposed a one-step HBM including three off-step points for the solution of general fourth-order ODEs. All these methods were limited to solving IVPs only. Mebarek-Oudina[28-33] solved, numerically, the differential equations of the fluid problem using the finite volume method. Raza et al[34,35] efficiently solved the fluid flow problems in a channel with three-stage Lobatto III-A formula method.

The introduction of a high-derivative approach is rarely seen in the literature of block methods. Jator and Li[36] introduced an algorithm for second-order IVPs and boundary value problems (BVPs) with an automatic error estimate based on a third derivative method (TDM) with continuous coefficients, which are simultaneously applied to provide all approximations on the entire interval. In addition, Jator et al[37] examined a case of high-order continuous third derivative formulas for second-order ODEs. In the same year, Sahi et al[38] developed a fourth-derivative method (FDM) with continuous coefficients to obtain primary and additional methods that are used to solve third-order boundary value problems (TOBVPs). Likewise, Adeyeye and Omar[39] suggested an HBM of order eight with the third derivative for solving second-order IVPs of ODEs. However, they did not establish a generalized high-derivative method for a second- or third-order IVPs, and the accuracy of these methods was not greatly encouraging.

On the basis of these previous works, we will attempt to develop a one-step HBM for solving BVPs of second-order ODEs, directly, using a collocation and interpolation approach in the presence of a third derivative.

2 | PROBLEM FORMULATION

Consider a longitudinal fin with a cross-sectional area A, length L, thermal conductivity k, and heat generation q_n. Moreover, the fin is in contact with a heated surface T_b, and loses heat to the surrounding medium with temperature T_1 over an invariant convective heat transfer coefficient h. Furthermore, it is assumed that heat conduction occurs only in the direction of the x-axis, as shown in Figure 1.

2.1 | Solid fin with temperature-dependent internal heat generation

For this problem, the governing differential equation and boundary conditions can be written as[6]

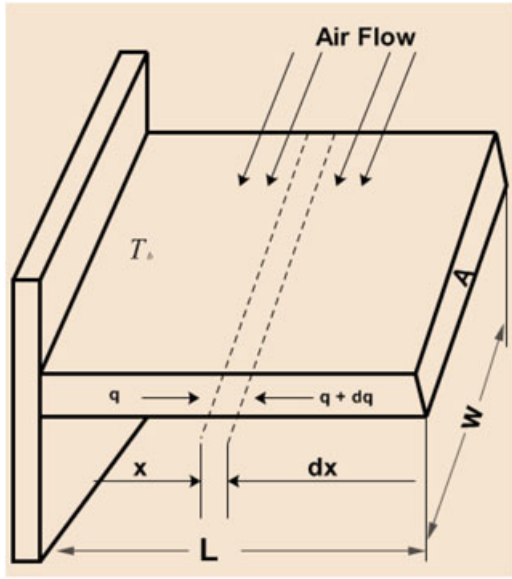

FIGURE 1 Physical sketch of the problem [Color figure can be viewed at wileyonlinelibrary.com]

$$\frac{d^2T}{dx^2} - \frac{hP}{kA}(T - T_\infty) + \frac{q^*}{k} = 0, \tag{1}$$

$$x = 0, \ \frac{dT}{dx} = 0, \tag{2}$$

$$x = L, T = T_b. \tag{3}$$

Consider that the heat generation in the fin varies with temperature as shown in Equation (4) and the thermal conductivity is constant $k_\circ$

$$q^* = q^*_\infty(1 + \epsilon(T - T_\infty)), \tag{4}$$

where q^*_∞ is the internal heat generation at temperature T_∞. Introduce the dimensionless variables as

$$\theta = \frac{T - T_\infty}{T_b - T_\infty}, \quad X = \frac{x}{L}, \quad G = \frac{q^*A}{hP(T_b - T_\infty)}, \quad N^2 = \frac{hPL^2}{k_\circ A}, \quad \epsilon_G = \epsilon(T_b - T_\infty).$$

So Equations (1)–(3) become

$$\frac{d^2\theta}{dX^2} - N^2\theta + N^2G(1 + \epsilon_G\theta) = 0. \tag{5}$$

Subject to the boundary conditions

$$X = 0, \quad \frac{d\theta}{dX} = 0, \tag{6}$$

$$X = 1, \ \theta = 1. \tag{7}$$

2.2 | Porous fin with temperature-dependent internal heat generation

Consider a porous fin such that the energy equation for this case becomes:

$$q(x) - q(x + \Delta x) + q^* \cdot A \cdot \Delta x = mc_p[T(x) - T_\infty] + h(p \cdot \Delta x)[T(x) - T_\infty]. \tag{8}$$

Use the rate of mass flow of the fluid through porous material $\dot{m} = \rho V_w \Delta x w$ and Darcy's model $V_W = gK\beta(T - T_\infty)/v$ in Equation (7) and use $\Delta x \to 0$, so we get:

$$\frac{dq}{dx} + q^* A = \frac{\rho C_p g K \beta w}{v}[T(x) - T_\infty]^2 + hp[T(x) - T_\infty]. \tag{9}$$

From Fourier's law of conduction

$$q = -k_{\text{eff}} A \frac{dT}{dx}, \tag{10}$$

where A is the cross-sectional area of the fin $A = wt$ and k_{eff} is the effective thermal conductivity of the porous fin and is defined as:

$$k_{\text{eff}} = \varphi k_f + (1 - \varphi) k_s. \tag{11}$$

Using the last two equations into the previous third and using the following dimensionless parameters:

$$\theta = \frac{T - T_\infty}{T_b - T_\infty}, \ X = \frac{x}{L}, \ G = \frac{q^* A}{hP(T_b - T_\infty)}, \ N^2 = \frac{hPL^2}{k_0 A}, \ \epsilon_G = \epsilon(T_b - T_\infty).$$

Then, we get:

$$\frac{d^2\theta}{dX^2} - N^2\theta + N^2 G(1 + \epsilon_G \theta) - S_h \theta^2 = 0. \tag{12}$$

Subject to the boundary conditions:

$$\theta(0) = 1, \ \frac{d\theta}{dX} = 0 \ \text{ at } \ x = 1, \tag{13}$$

where S_h is the porosity parameter and N is the convection parameter.

3 | DEVELOPMENT OF HBD

To derive the method of Equation (1) subject to the boundary conditions (6) and (7), we consider

$$y'' = f(x, y, y') = N^2\theta - N^2G(1 + \epsilon_G\theta)\ ,\ x \in [a, b], y(a) = \alpha, y(b) = \beta. \tag{14}$$

Employ the following power series to provide Equation (14) with the approximate numerical solution:

$$y(x) = \sum_{i=0}^{2\vartheta+\theta-1} c_i\left(\frac{x - x_n}{h}\right)^i, \tag{15}$$

where θ and ϑ refer to the interpolation and collocation points respectively. Evaluating the second and third derivatives of Equation (14), the following two equations are obtained:

$$y''(x) = \sum_{i=0}^{2\vartheta+\theta-1} \frac{i!ac_i}{h^2(i-2)!}\left(\frac{x - x_n}{h}\right)^{i-2} = f(x, y, y'), \tag{16}$$

$$y'''(x) = \sum_{i=0}^{2\vartheta+\theta-1} \frac{i!c_j}{h^3(i-3)!}\left(\frac{x - x_n}{h}\right)^{i-3} = g(x, y, y'). \tag{17}$$

Then, Equation (15) is interpolated at the points $x_{n+\hat{\theta}}$, for $\hat{\theta} = \{0,3/5\}$ and Equations (16) and (17) are collocated at all points $x_{n+\hat{\vartheta}}$, for $\hat{\vartheta} = \{0,2/5,\ 3/5,1\}$, respectively. Then, combine the resulting equations in a matrix form:

$$A = \begin{pmatrix}
1 & 0 & 0 & 0 & 0 & 0 & 0 & 0 & 0 & 0 \\
1 & \frac{2}{5} & \frac{4}{25} & \frac{8}{125} & \frac{16}{625} & \frac{32}{3125} & \frac{64}{15625} & \frac{128}{78125} & \frac{1511157274518287}{2305843009213693952} & \frac{4835703278458519}{18446744073709551616} \\
0 & 0 & \frac{2}{h^2} & 0 & 0 & 0 & 0 & 0 & 0 & 0 \\
0 & 0 & \frac{2}{h^2} & \frac{12}{5h^2} & \frac{48}{25h^2} & \frac{32}{25h^2} & \frac{96}{125h^2} & \frac{1344}{3125h^2} & \frac{3584}{15625h^2} & \frac{9216}{78125h^2} \\
0 & 0 & \frac{2}{h^2} & \frac{18}{5h^2} & \frac{108}{25h^2} & \frac{108}{25h^2} & \frac{486}{125h^2} & \frac{10206}{3125h^2} & \frac{40824}{15625h^2} & \frac{157464}{78125h^2} \\
0 & 0 & \frac{2}{h^2} & \frac{6}{h^2} & \frac{12}{h^2} & \frac{20}{h^2} & \frac{30}{h^2} & \frac{42}{h^2} & \frac{56}{h^2} & \frac{72}{h^2} \\
0 & 0 & 0 & \frac{6}{h^3} & 0 & 0 & 0 & 0 & 0 & 0 \\
0 & 0 & 0 & \frac{6}{h^3} & \frac{48}{5h^3} & \frac{48}{5h^3} & \frac{192}{25h^3} & \frac{672}{125h^3} & \frac{10752}{3125h^3} & \frac{32256}{15625h^3} \\
0 & 0 & 0 & \frac{6}{h^3} & \frac{72}{5h^3} & \frac{108}{5h^3} & \frac{648}{25h^3} & \frac{3402}{125h^3} & \frac{81648}{3125h^3} & \frac{367416}{15625h^3} \\
0 & 0 & 0 & \frac{6}{h^3} & \frac{24}{h^3} & \frac{60}{h^3} & \frac{120}{h^3} & \frac{210}{h^3} & \frac{336}{h^3} & \frac{504}{h^3}
\end{pmatrix}$$

$$B = (a_0 a_1 a_2 a_3 a_4 a_5 a_6 a_7 a_8 a_9)^T$$

$$X = (y_n y_{n+\frac{2}{5}} f_n f_{n+\frac{2}{5}} f_{n+\frac{3}{5}} f_{n+1} g_n g_{n+\frac{2}{5}} g_{n+\frac{3}{5}} g_{n+1})^T$$

The unknown values a_i′s resulting from solving the system $AX = B$ using matrix inversion are listed in Appendix (A). Now, substituting the values of a_i′s back into Equation (15) produces a linear multistep continuous hybrid scheme of the form:

$$y(x) = \sum_{j=0,\frac{2}{5}} \alpha_j y_{n+j} + h^2 \sum_{j=0,\frac{2}{5},\frac{3}{5},1} \beta_j f_{n+j} + h^3 \sum_{j=0,\frac{2}{5},\frac{3}{5},1} \gamma_j g_{n+j}, \tag{18}$$

where the coefficients α_0, α_1, β_j and γ_j for $j = \left\{0, \frac{2}{5}, \frac{3}{5}, 1\right\}$ are listed in Appendix (B).

Now, on deriving Equation (18) once we obtain:

$$y'(x) = \frac{1}{h} \sum_{j=0,\frac{3}{5}} \alpha'_j y_{n+j} + h \sum_{j=0,\frac{3}{5},1} \beta'_j f_{n+j} + h^2 \sum_{j=0,\frac{3}{5},1} \gamma'_j g_{n+j}, \tag{19}$$

After that, Equation (18) is evaluated at the points $x_{n+\frac{3}{5}}$ and x_{n+1}, while Equation (19) is evaluated at all points $x_{n+\frac{i}{5}}$, for $i = \{0, 2, 3, 5\}$, which produces the following main block:

$$E^{(0)} Y_{p+1} = h E^{(1)} Y_p + h^2 \sum_{i=0}^{1} R^{(i)} F_{p+i} + h^3 \sum_{i=0}^{1} K^{(i)} G_{p+i}, \tag{20}$$

where

$$E^{(0)} = \begin{pmatrix} 1 & 0 & 0 \\ 0 & 1 & 0 \\ 0 & 0 & 1 \end{pmatrix}, \quad E^{(1)} = \begin{pmatrix} 0 & 0 & \frac{2}{5} \\ 0 & 0 & \frac{3}{5} \\ 0 & 0 & 1 \end{pmatrix}, \quad R^{(0)} \begin{pmatrix} 0 & 0 & \frac{47631028758991}{1108307720798208} \\ 0 & 0 & \frac{8928152074081389}{126100789566373888} \\ 0 & 0 & \frac{9811091788226625536}{76606229661572140625} \end{pmatrix},$$

$$R^{(1)} = \begin{pmatrix} \frac{-693179042646125}{11399736556781568} & \frac{23445811717684840103936}{24513993491703071289062 5} & \frac{523714593467660238848}{23939446769241293945312 5} \\ \frac{-5003481171610111574016}{61284983729257666015625} & \frac{747}{4000} & \frac{979396966539331633152}{23939446769241293945312 5} \\ \frac{-46116860184268}{1255116466775197} & \frac{278348191826528}{717209409585827} & \frac{100862617254584}{4902798698340617} \end{pmatrix},$$

$$K^{(0)}\begin{pmatrix} 0 & 0 & \frac{13886}{8859375} \\ 0 & 0 & \frac{9423}{3500000} \\ 0 & 0 & \frac{461}{90720} \end{pmatrix}, \quad K^{(1)} = \begin{pmatrix} \frac{-6004}{354375} & \frac{-3196}{354375} & \frac{-1684}{8859375} \\ \frac{-4563}{140000} & \frac{-603}{35000} & \frac{-621}{1750000} \\ \frac{-1025}{18144} & \frac{-25}{1296} & \frac{-31}{22680} \end{pmatrix}.$$

$$Y_{p+1} = \left[y_{n+\frac{2}{5}}, y_{n+\frac{3}{5}}, y_{n+1}\right]^T, \; Y_p = \left[y_{n-\frac{3}{5}}, y_{n-\frac{2}{5}}, y_n\right]^T,$$

$$F_{p+1} = \left[f_{n+\frac{2}{5}}, f_{n+\frac{3}{5}}, f_{n+1}\right]^T, \; F_p = \left[f_{n-\frac{3}{5}}, f_{n-\frac{2}{5}}, f_n\right]^T,$$

$$G_{p+1} = \left[g_{n+\frac{2}{5}}, g_{n+\frac{3}{5}}, g_{n+1}\right]^T, \quad \text{and} \quad G_p = \left[g_{n-\frac{3}{5}}, g_{n-\frac{2}{5}}, g_n\right]^T.$$

The derivative of the main block (20) is given below:

$$E^{(0)}\hat{Y}_{p+1} = \tilde{E}^{(1)}\hat{Y}_p + h\sum_{i=0}^{1} \tilde{R}^{(i)}\hat{F}_{p+i} + h^2\sum_{i=0}^{1} \tilde{K}^{(i)}\hat{G}_{p+i}, \tag{21}$$

$$\tilde{E}^{(1)} = \begin{pmatrix} 0 & 0 & 1 \\ 0 & 0 & 1 \\ 0 & 0 & 1 \end{pmatrix}, \quad \tilde{R}^{(0)} = \begin{pmatrix} 0 & 0 & \frac{16417}{118125} \\ 0 & 0 & \frac{19497}{140000} \\ 0 & 0 & \frac{899}{6048} \end{pmatrix},$$

$$\tilde{R}^{(1)} = \begin{pmatrix} \frac{-3088718744438125}{17732923532771328} & \frac{4639356134537952231424}{10895108218534697265625} & \frac{1108}{118125} \\ \frac{-4867778707638183788544}{65370649311208193359375} & \frac{4141904282296875}{7881299347898368} & \frac{1353}{140000} \\ \frac{2351959869397632}{6693954489467719} & \frac{1224979098644774912}{3486434629931103125} & \frac{189784503047153125}{1276770494359535616} \end{pmatrix},$$

$$\tilde{K}^{(0)} = \begin{pmatrix} 0 & 0 & \frac{221}{39375} \\ 0 & 0 & \frac{789}{140000} \\ 0 & 0 & \frac{13}{2016} \end{pmatrix}, \quad \tilde{K}^{(1)}\begin{pmatrix} \frac{-211}{2625} & \frac{-104}{2625} & \frac{-32}{39375} \\ \frac{-2151}{28000} & \frac{-1209}{28000} & \frac{-117}{140000} \\ \frac{-25}{672} & \frac{25}{672} & \frac{-13}{2016} \end{pmatrix}.$$

$$\hat{Y}_{p+1} = \left[y'_{n+\frac{2}{5}}, y'_{n+\frac{3}{5}}, y'_{n+1}\right]^T, \hat{Y}_p = \left[y'_{n-\frac{3}{5}}, y'_{n-\frac{2}{5}}, y'_n\right]^T,$$

$$\hat{F}_{p+1} = \left[f'_{n+\frac{2}{5}}, f'_{n+\frac{3}{5}}, f'_{n+1}\right]^T, \hat{F}_p = \left[f'_{n-\frac{3}{5}}, f'_{n-\frac{2}{5}}, f'_n\right]^T,$$

$$\hat{G}_{p+1} = \left[g'_{n+\frac{2}{5}}, g'_{n+\frac{3}{5}}, g'_{n+1}\right]^T, \quad \text{and} \quad \hat{G}_p = \left[g'_{n-\frac{3}{5}}, g'_{n-\frac{2}{5}}, g'_n\right]^T.$$

3.1 | Analysis of the one-step third derivative HBD

In this section, we discuss the zero-stability, order, consistency, convergence, and region of absolute stability of the one-step third derivative HBD.

3.1.1 | Zero stability

The zero-stability property of the HBD Formula (21) is satisfied if all roots (r_z) of the first characteristic equation $\rho(r)$ are inside the unit circle and if $r_z = 1$. Then, the multiplicity of (r_z) must not exceed two.

$$\det[rE^{(0)} - E^{(1)}] = \left| r\begin{pmatrix} 1 & 0 & 0 \\ 0 & 1 & 0 \\ 0 & 0 & 1 \end{pmatrix} - \begin{pmatrix} 0 & 0 & \frac{2}{5} \\ & & \\ 0 & 0 & \frac{3}{5} \\ & & \\ 0 & 0 & 1 \end{pmatrix} \right| = 0$$

Implies: $r^2(r-1) = 0$
Moreover, $r = 0,0,1$. Thus, Equation ((21)) fulfills the zero-stability condition.

3.1.2 | Order of the method

According to Jator and Li,[36] the HBD Formula (20) possesses an order q if the linear operator π associated with the block can be expressed as

$$\pi\{y(x), h\} = \sum_{i=0}^{1} (-1)^i E^{(i)} Y_{p+1-i} - \sum_{i=0}^{1} R^{(i)} F_{p+i} - \sum_{i=0}^{1} K^{(i)} G_{p+i}. \tag{22}$$

Using Taylor series expansion and gathering similar terms

$$\pi\{y(x), h\} = \sum_{i=0}^{\infty} \hat{D}_i h^i y^{(i)} = 0\,, \tag{23}$$

where

$$\hat{D}_0 = \hat{D}_1 = \hat{D}_2 = \ldots = \hat{D}_{q+1} = 0 \quad \text{and } \hat{D}_{q+2} \neq 0.$$

The term $\hat{C}_{q+2}$ is called the error constant and the local truncation error is given by

$$t_k = \hat{D}_{q+2} h^{n+2} y^{n+2} + O(h^{n+3}).$$

Comparing the coefficients of $y^{(i)}$ and h^i produce $\hat{D}_0 = \hat{D}_1 = \hat{D}_2 = ... = \hat{D}_9 = 0$, with a vector of error constants

$$\hat{D}_{10} = [2.3233e^{-10}, 4.2759e^{-10}, 9.7632e^{-10}]^T,$$

which concludes that the order (q) of this algorithm is 8.

3.1.3 | Consistency

Definition 3.2. A HBD is said to be consistent if $(q \geq 1)$, that is, the order is greater than one.

From the analysis shown above for the HBD (20), we conclude that the order exceeds one. Thus, the HBD is consistent.

3.1.4 | Convergence

Theorem 3.1. *Referring to Henrici,[40] a linear multistep method is convergent if it is consistent and zero-stable.*

The HBD Formula (20) is convergent as it fulfills both the consistency and zero-stability conditions.

3.1.5 | Absolute stability

Considering the methods of the block (13), the stability region is discussed in Jator et al.[37]

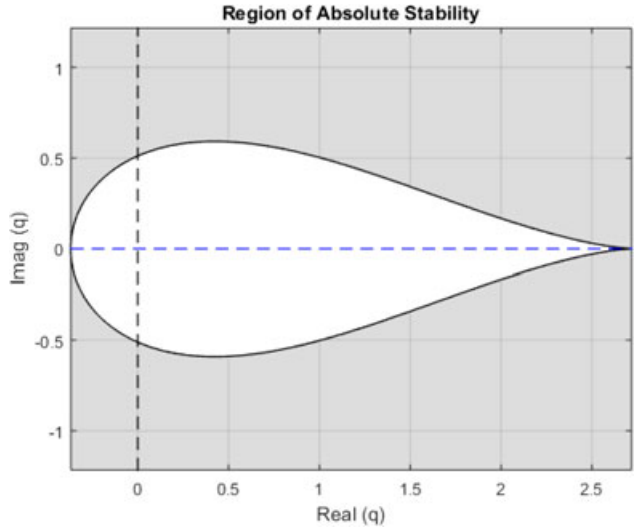

FIGURE 2 Region of absolute stability [Color figure can be viewed at wileyonlinelibrary.com]

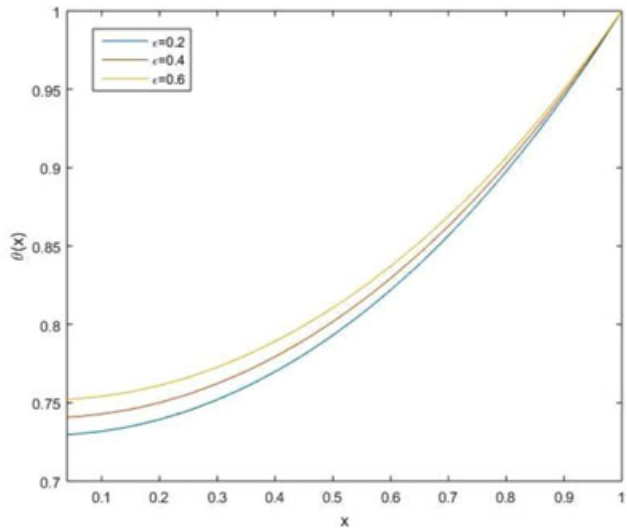

FIGURE 3 Temperature distribution in the fin for the variation of ϵ_G [Color figure can be viewed at wileyonlinelibrary.com]

Then, the test problem of the form $y' = \mu y$, $y'' = \mu^2 y$ and $y''' = \mu^3 y$ are substituted into Equation (23) to yield:

$$\hat{Y}_{p+1} = M(w)\hat{Y}_p, \tag{24}$$

where $v = \mu h$ and

$$M(v) = (E^{(0)} - v^2 R^{(1)} - v^3 K^{(1)})^{-1}(vE^{(1)} + v^2 R^{(0)} + v^3 K^{(0)}).$$

Calculating the eigenvalues for the matrix $M(v)$ produces only one nonzero value, namely μ. Thus, the region of absolute stability is depicted in the Figure 2.

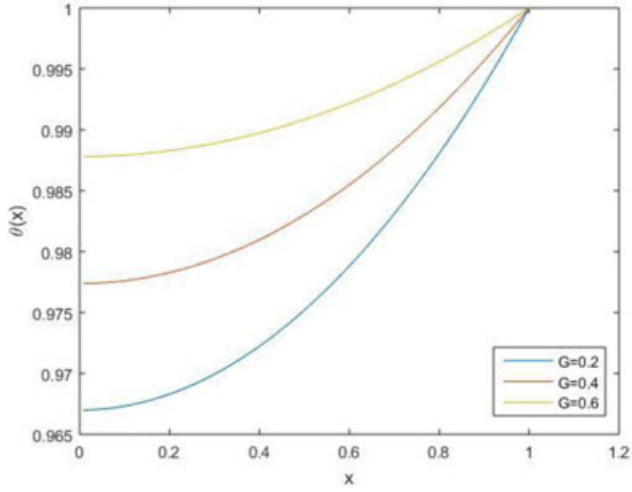

FIGURE 4 Temperature distribution in the fin for the variation of G [Color figure can be viewed at wileyonlinelibrary.com]

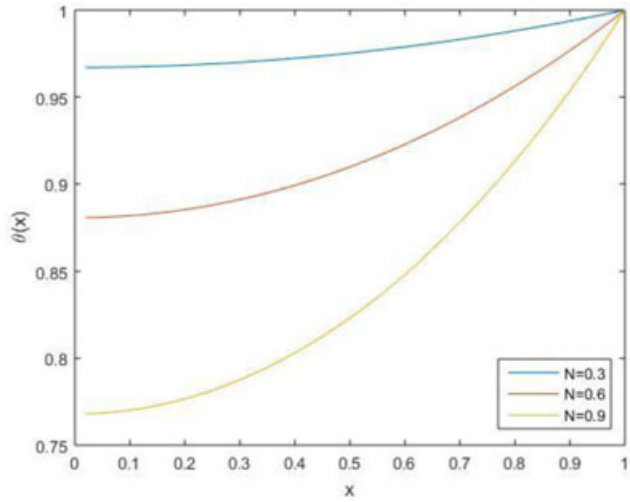

FIGURE 5 Temperature distribution in the fin for the variation of N [Color figure can be viewed at wileyonlinelibrary.com]

4 | RESULTS AND DISCUSSION

The current section presents the numerical results in the form of pictorial representation. Figures 3-6 indicate the numerical results of the first case. Figure 3 shows the effect of temperature distribution in the fin for the variation of ϵ_G. The choice of parameter $\epsilon_G = 0.2, 0.4, 0.6$ shows that a fin with moderate temperature-dependent heat generation and the thermal conductivity variation of 20% between the base and the surrounding coolant temperatures that are often used in nuclear rods Ghasemi et al.[41] Furthermore, it is noticed that the temperature profile increases monotonically with the enhancement of the strength of ϵ_G. From the physical point of view, we can say that the temperature of the fin increases due to the increase in the heat generation. Figure 4 elucidates the effects of G on temperature distribution

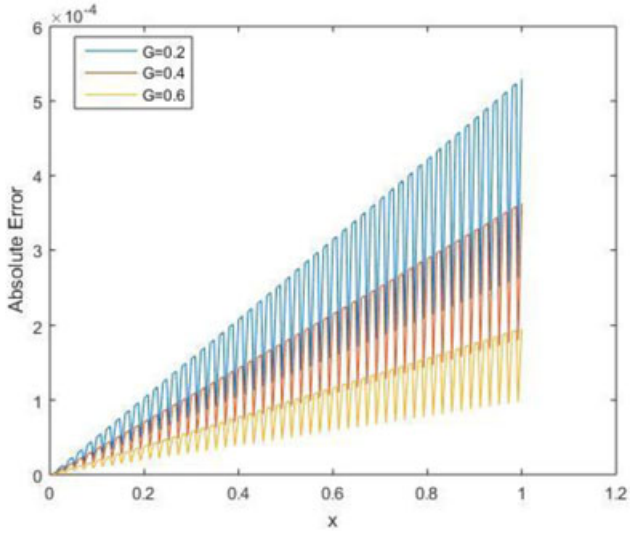

FIGURE 6 Error of hybrid block method for successive iterations [Color figure can be viewed at wileyonlinelibrary.com]

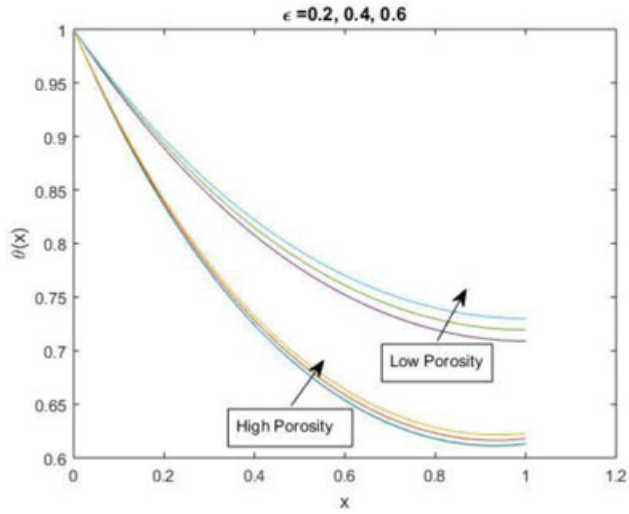

FIGURE 7 Temperature distribution in a porous fin for the variation of ϵ_G [Color figure can be viewed at wileyonlinelibrary.com]

in the fin. The temperature profile rises gradually for the variations of $G = 0.2, 0.4, 0.6$, due to the increase in heat generation. The effect of different values of N on temperature distribution is presented in Figure 5. The choice of $N = 0.3, 0.6, 0.9$ is used in compact heat exchanger fin design. The temperature profile drops monotonically for the variations of N. The error of the proposed numerical method for the variations of $G = 0.2, 0.4, 0.6$ is also plotted in Figure 6. It is seen that maximum error occurs at the tip of the solid fin.

Figures 7-10 are plotted for the second case considered in this problem. The effect of the thermal conductivity parameter $\epsilon_G = 0.2, 0.4, 0.6$ on temperature distribution is presented in Figure 7. It is depicted from this plot that the profile for temperature distribution rises monotonically with enhancement in the strength of the heat generation parameter ϵ_G, both for the case of high porosity as well as that of low porosity. Moreover, it is seen that the profile of

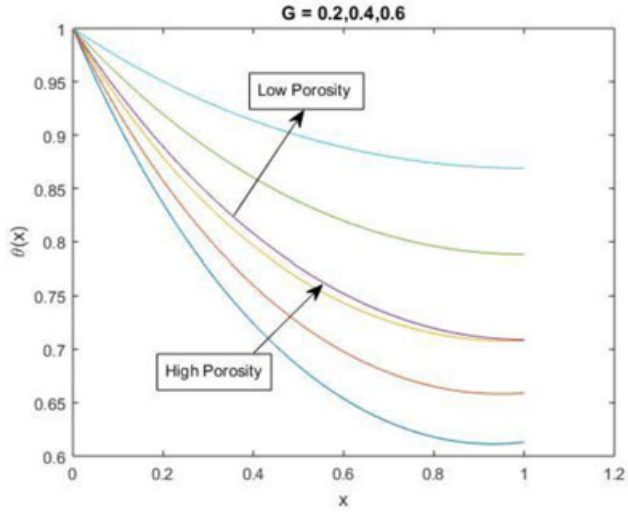

FIGURE 8 Temperature distribution in a porous fin for the variation of G [Color figure can be viewed at wileyonlinelibrary.com]

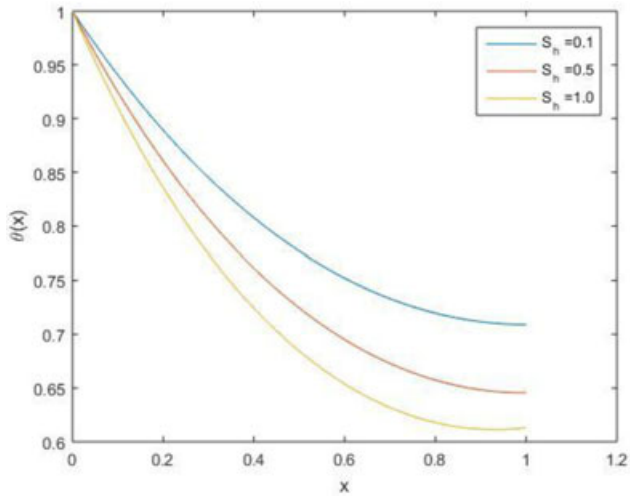

FIGURE 9 Temperature distribution in the porous fin for the variation of S_h [Color figure can be viewed at wileyonlinelibrary.com]

low porosity is much higher than the high porosity rate. This is due to the collision between the fluid particles and the pores of the porous screen.

The same phenomenon is seen for the variations of $G = 0.2, 0.4, 0.6$ in Figure 8. The error of the proposed numerical method for the variations of $\epsilon_G = 0.2, 0.4, 0.6$ is also plotted in Figure 10. It is depicted that maximum error occurs at the bottom of the porous fin.

The effect of the porosity parameter on temperature distribution is elucidated in Figure 9. It is clearly seen that the temperature distribution profile drops gradually as the porosity parameter changes from low to high. The porosity parameter actually depends upon the Darcy number $D_a = k/t^2$; therefore, we can say that the permeability of the fin decreases as the Darcy number reduces. In addition, considering the permeability definition, if the increases of the permeable media are small or in the event that they are ineffectively associated, the porosity will be low and the fluid

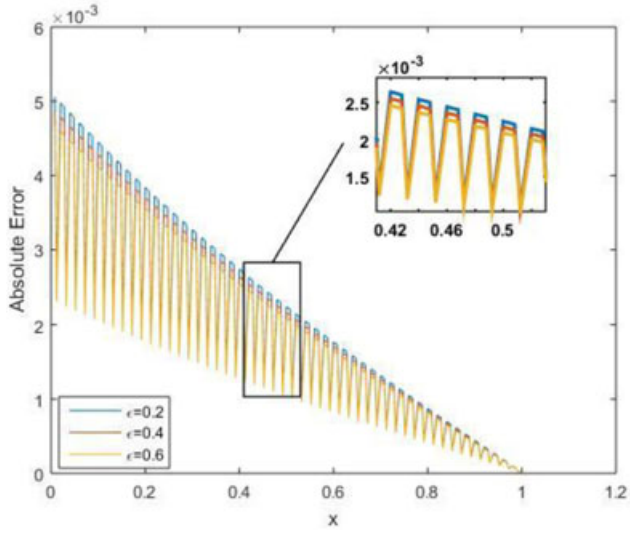

FIGURE 10 Error of hybrid block method for successive iterations [Color figure can be viewed at wileyonlinelibrary.com]

will not flow through effectively. In this way, when the Darcy number and, therefore, the porosity diminishes, the crash between the fluid flow and the pores of the permeable screen increments. In this manner, the passing fluids give more space to contact with the permeable media, which have inward heat generation. Therefore, the estimation of the temperature is expanded by diminishing the D_a number. Then again, S_h is associated specifically to D_a number variation.

5 | CONCLUSION

A successful derivation of a one-step HBD of order (8) incorporating two off-step points in the presence of a third derivative is presented. In addition, the developed method is used to solve second-order BVPs of ODEs directly for the Dirichlet and mixed cases. The numerical analysis presented reveals that the proposed method is not only consistent but also zero-stable, which concludes that it is convergent beside a significant interval of absolute stability, making it a suitable candidate for solving general ODEs. The graphs and tables shown above illustrate the superiority of the numerical results.

NOMENCLATURE

A	Cross-sectional area (m^2)
g	Acceleration($m{\cdot}s^{-2}$)
$\boldsymbol{p}$	Pressure (Pa)
K	Permeability (m^2)
k	Thermal conductivity of the fluid (W/m·K)
k_{eff}	Effective thermal conductivity of the porous fin (W/m·K)
h	Convective heat transfer coefficient($W/m^2{\cdot}K$)
L	Length (m)
$\dot{m}$	Rate of mass flow of the fluid(Kg/s)
q_n	Heat generation (J)
q^*_∞	Internal heat generation (J)
$\boldsymbol{T}$	Fluid temperature (K or °C)
v_w	Uniform velocity
c_p	Specific heat at constant pressure (J/kg·K)
(u, v)	Velocity component in Cartesian co-ordinate

GREEK SYMBOLS

$\boldsymbol{\beta}$	Thermal expansion coefficient of the fluid (K^{-1})
$\boldsymbol{\mu}$	Dynamic viscosity (Pa·s)
$\boldsymbol{\theta}$	Dimensionless temperature
ρ	Density (kg/m^3)

DIMENSIONLESS NUMBERS

D_a	Darcy number
Pr	Prandtl number

N Convection parameter
G Heat generation parameter
S_h Porosity parameter

ORCID

Fateh Mebarek-Oudina http://orcid.org/0000-0001-6145-8195
Jawad Raza http://orcid.org/0000-0002-6877-805X

REFERENCES

1. Kraus AD, Aziz A, Welty JR. *Extended Surface Heat Transfer*. New York, NY: John Wiley; 2002.
2. Hatami M, Ganji DD. Investigation of refrigeration efficiency for fully wet circular porous fins with variable sections by combined heat and mass transfer analysis. *Int J Refrig*. 2014;40:140-151.
3. Hatami M, Ganji DD. Thermal behavior of longitudinal convective-radiative porous fins with different section shapes and ceramic materials (SiC and Si3N4). *Ceramics Int*. 2014;40(5):6765-6775.
4. Ghasemi SE, Hatami M, Ganji DD. Thermal analysis of convective fin with temperature-dependent thermal conductivity and heat generation. *Case Studies Therm Eng*. 2014;4:1-8.
5. Atouei SA, Hosseinzadeh K, Hatami M, Ghasemi SE, Sahebi SAR, Ganji DD. Heat transfer study on convective-radiative semi-spherical fins with temperature-dependent properties and heat generation. *Appl Therm Eng*. 2015;89:299-305.
6. Aziz A, Bouaziz MN. A least squares method for a longitudinal fin with temperature dependent internal heat generation and thermal conductivity. *Energy Conver Manage*. 2011;52:2876-2882.
7. Razani A, Ahmadi G. On optimization of circular fins with heat generation. *J Franklin Inst*. 1977;303(2):211-218.
8. Ünal HC. Temperature distributions in fins with uniform and non-uniform heat generation and non-uniform heat transfer coefficient. *Int J Heat Mass Transfer*. 1987;30(7):1465-1477.
9. Ghadikolaei SS, Hosseinzadeh K, Yassari M, Sadeghi H, Ganji DD. Analytical and numerical solution of non-Newtonian second-grade fluid flow on a stretching sheet. *Therm Sci Eng Prog*. 2018;5:309-316.
10. Ardahaie SS, Amiri AJ, Amouei A, Hosseinzadeh K, Ganji DD. Investigating the effect of adding nanoparticles to the blood flow in presence of magnetic field in a porous blood arterial. *Inform Med Unlocked*. 2018;10:71-81.
11. Hosseinzadeh K, Amiri AJ, Ardahaie SS, Ganji DD. Effect of variable lorentz forces on nanofluid flow in movable parallel plates utilizing analytical method. *Case Studies Therm Eng*. 2017;10:595-610.
12. Ghadikolaei SS, Hosseinzadeh K, Ganji DD. Analysis of unsteady MHD Eyring-Powell squeezing flow in stretching channel with considering thermal radiation and Joule heating effect using AGM. *Case Studies Therm Eng*. 2017;10:579-594.
13. Rahimi J, Ganji DD, Khaki M, Hosseinzadeh K. Solution of the boundary layer flow of an Eyring-Powell non-Newtonian fluid over a linear stretching sheet by collocation method. *Alexandria Eng J*. 2017;56(4):621-627.
14. Shouman AR, Nonlinear heat transfer and temperature distribution through fins and electric filaments of arbitrary geometry with temperature-dependent properties and heat generation, NASA technical note, TN D-4257; 1968.
15. Kundu B. Performance and optimum design analysis of longitudinal and pin fins with simultaneous heat and mass transfer: unified and comparative investigations. *Appl Therm Eng*. 2007;27:976-987.
16. Domairry G, Fazeli M. Homotopy analysis method to determine the fin efficiency of convective straight fins with temperature-dependent thermal conductivity. *Commun Nonlin Sci Num Simul*. 2009;14(2):489-499.
17. Ganji DD, Ganji ZZ, Ganji HD. Determination of temperature distribution for annular fins with temperature-dependent thermal conductivity by HPM. *Therm Sci*. 2011;15(Suppl 1):111-115.
18. Aziz A, Khani F. Convection–radiation from a continuously moving fin of variable thermal conductivity. *J Franklin Inst*. 2011;348(4):640-651.
19. Bouaziz MN, Aziz A. Simple and accurate solution for convective-radiative fin with temperature-dependent thermal conductivity using double optimal linearization. *Energy Convers Manage*. 2010;51(12):2776-2782.

20. Kayode S, Adeyeye O. A 3-step hybrid method for direct solution of second order initial value problems. *Aust J Basic Appl Sci*. 2011;5(12):2121-2126.
21. Badmus A. An efficient seven-point hybrid block method for the direct solution of y″ = f (x,y,y'). *British J Math Comp Sci*. 2014;4(19):2840-2852.
22. Kuboye JO, Omar Z. Numerical solution of third order ordinary differential equations using a seven-step block method. *Int J Math Anal*. 2015;9(15):743-745.
23. Anake T, Awoyemi DO, Adesanya A. One-step implicit hybrid block method for the direct solution of general second order ordinary differential equations. *Int J Appl Math*. 2012;42(4):1-5.
24. Adeyeye O. Two-step two-point hybrid methods for general second order differential equations. *African J Math Comp Sci Res*. 2013;6(10):191-196.
25. Omar Z, Abdelrahim R. Developing a single-step hybrid block method with generalized three off-step points for the direct solution of second order ordinary differential equations. *Int J Math Anal*. 2015;9(46):2257-2272.
26. Abdelrahim R, Omar Z. Uniform order one-step hybrid block method with two generalized off-step points for solving third order ordinary differential equations directly. *Global J Pure Appl Math*. 2015;11(6):4809-4823.
27. Omar Z, Abdelrahim R. Direct solution of fourth-order ordinary differential equations using a one-step hybrid block method of order five. *Int J Pure Appl Math*. 2016;109(4):763-777.
28. Mebarek-Oudina F, Bessaïh R. Numerical modeling of MHD stability in a cylindrical configuration. *J Franklin Inst*. 2014;351(2):667-681.
29. Mebarek-Oudina F, Bessaïh R. Oscillatory magnetohydrodynamic natural convection of liquid metal between vertical coaxial cylinders. *J Appl Fluid Mech*. 2016;9(4):1655-1665.
30. Mebarek-Oudina F. Numerical modeling of the hydrodynamic stability in vertical annulus with heat source of different lengths. *Eng Sci Technol*. 2017;20(4):1324-1333.
31. Mebarek-Oudina F, Makinde OD. Numerical simulation of oscillatory MHD natural convection in cylindrical annulus: Prandtl number effect. *Defect Diff Forum*. 2018;387:417-427.
32. Mebarek-Oudina F. Convective heat transfer of titania nanofluids of different base fluids in cylindrical annulus with discrete heat source. *Heat Trans–Asian Res*. 2019;48:135-147.
33. Mebarek-Oudina F, Bessaih R. Oscillatory mixed convection flow in a cylindrical container with rotating disk under axial magnetic field and various wall electrical conductivity. *Int Rev Phys*. 2010;4(1):45-51.
34. Reza J, Mebarek-Oudina F, Makinde OD. MHD slip flow of Cu-Kerosene nanofluid in a channel with stretching walls using 3-stage Lobatto IIIA formula. *Defect Diff Forum*. 2018;387:51-62.
35. Raza J, Mebarek-Oudina F, Chamkha AJ. Magnetohydrodynamic flow of molybdenum disulfide nanofluid in a channel with shape effects. *Multidisc Model Mater Struct*. 2019. https://doi.org/10.1108/MMMS-07-2018-0133
36. Jator SN, Li J. An algorithm for second order initial and boundary value problems with an automatic error estimate based on a third derivative method. *Num Algorithm*. 2012;59(3):333-346.
37. Jator SN, Akinfenwa AO, Okunuga SA, Sofoluwe AB. High-order continuous third derivative formulas with block extensions for y″ = f (x,y,y′). *Int J Comput Math*. 2013;90(9):1899-1914.
38. Sahi RK, Jator SN, Khan NA. Continuous fourth derivative method for third-order boundary value problems. *Int J Pure Appl Math*. 2013;85(5):907-923.
39. Adeyeye O, Omar Z. New uniform order eight hybrid third derivative block method for solving second order initial value problems. *Far East J Math Sci*. 2016;100(9):1515-1531.
40. Henrici P. *Discrete Variable Methods in Ordinary Differential Equations*. New York, NY: John Wiley and Sons; 1962.
41. Ghasemi SE, Valipour P, Hatami M, Ganji DD. Heat transfer study on solid and porous convective fins with temperature-dependent heat generation using efficient analytical method. *J Central South Univ*. 2014;21(12):4592-4598.

How to cite this article: Alkasassbeh M, Omar Z, Mebarek-Oudina F, Raza J, Chamkha A. Heat transfer study of convective fin with temperature-dependent internal heat generation by hybrid block method. *Heat Transfer—Asian Res*. 2019;1-20. https://doi.org/10.1002/htj.21428

APPENDIX A

$$a_0 = y_n,$$

$$a_1 = \frac{5}{2}y_{n+\frac{2}{5}} - \frac{5}{2}y_n - \frac{h^2}{374053855769395200000}\Big(40188680515398664192f_n + 2045760130733049472f_{n+1} - 56862343342063656000f_{n+\frac{2}{5}} + 89438673849810992000f_{n+\frac{3}{5}} + 146571057247656326 4hg_n - 17775144779277944 1hg_{n+1} - 15843522751601054400hg_{n+\frac{2}{5}} - 84336939896930352 00hg_{n+\frac{3}{5}}\Big),$$

$$a_2 = \frac{h^2 f_n}{2},$$

$$a_3 = \frac{h^3 g_n}{6},$$

$$a_4 = -\frac{h^2}{144}\Big(761f_n - 136f_{n+1} + 4375f_{n+\frac{2}{5}} - 5000f_{n+\frac{3}{5}} + 124hg_n + 12hg_{n+1} + 750hg_{n+\frac{2}{5}} + 500hg_{n+\frac{3}{5}}\Big),$$

$$a_5 = \frac{h^2}{2160}\Big(38191f_n - 11316f_{n+1} + 350625f_{n+\frac{2}{5}} - 377500f_{n+\frac{3}{5}} + 4683hg_n + 1008hg_{n+1} + 52875hg_{n+\frac{2}{5}} + 39000hg_{n+\frac{3}{5}}\Big),$$

$$a_6 = -\frac{5h^2}{648}\Big(3730f_n - 1630f_{n+1} + 46450f_{n+\frac{2}{5}} - 48550f_{n+\frac{3}{5}} + 408hg_n + 147hg_{n+1} + 6420hg_{n+\frac{2}{5}} + 5205hg_{n+\frac{3}{5}}\Big),$$

$$a_7 = \frac{25h^2}{1512}\Big(1574f_n - 949f_{n+1} + 24250f_{n+\frac{2}{5}} - 24875f_{n+\frac{3}{5}} + 162hg_n + 87hg_{n+1} + 3150hg_{n+\frac{2}{5}} + 2775hg_{n+\frac{3}{5}}\Big),$$

$$a_8 = -\frac{625h^2}{6048}\left(121f_n - 96f_{n+1} + 2175f_{n+\frac{2}{5}} - 2200f_{n+\frac{3}{5}} + 12hg_n + 9hg_{n+1} + 270hg_{n+\frac{2}{5}} + 255hg_{n+\frac{3}{5}}\right),$$

$$a_9 = -\frac{625h^2}{7776}\left(31f_n - 31f_{n+1} + 625f_{n+\frac{2}{5}} - 625f_{n+\frac{3}{5}} + 3hg_n + 3hg_{n+1} + 75hg_{n+\frac{2}{5}} + 75hg_{n+\frac{3}{5}}\right).$$

APPENDIX B

$$\alpha_0 = \frac{5}{2h}\left(\frac{2h}{5} - x - x_n\right),$$

$$\alpha_1 = \frac{5}{2h}(x - x_n),$$

$$\beta_0 = \frac{(x-x_n)^2}{2} - \frac{761}{144h^2}(x-x_n)^4 + \frac{38191}{2160h^3}(x-x_n)^5 - \frac{9325}{324h^4}(x-x_n)^6 + \frac{19675}{756h^5}(x-x_n)^7 - \frac{75625}{6048h^6}(x-x_n)^8 + \frac{19375}{7776h^7}(x-x_n)^9 - \frac{238155143794955h}{2216615441596416}(x-x_n),$$

$$\beta_{\frac{2}{5}} = -\frac{4375}{144h^2}(x-x_n)^4 + \frac{23375}{144h^3}(x-x_n)^5 - \frac{116125}{324h^4}(x-x_n)^6 + \frac{303125}{756h^5}(x-x_n)^7 - \frac{453125}{2016h^6}(x-x_n)^8 + \frac{390625}{7776h^7}(x-x_n)^9 + \frac{3465895213230625h}{22799473113563136}(x-x_n),$$

$$\beta_{\frac{3}{5}} = \frac{625}{18h^2}(x-x_n)^4 - \frac{18875}{108h^3}(x-x_n)^5 + \frac{121375}{324h^4}(x-x_n)^6 - \frac{621875}{1512h^5}(x-x_n)^7 + \frac{171875}{756h^6}(x-x_n)^8 - \frac{390625}{7776h^7}(x-x_n)^9 - \frac{11722905858842420051968}{49027986983406142578125}(x-x_n), + \frac{3465895213230625h}{22799473113563136}(x-x_n),$$

$$\beta_1 = \frac{17}{18h^2}(x-x_n)^4 - \frac{943}{180h^3}(x-x_n)^5 + \frac{4075}{324h^4}(x-x_n)^6 - \frac{23725}{1512h^5}(x-x_n)^7 + \frac{625}{63h^6}(x-x_n)^8 - \frac{19375}{7776h^7}(x-x_n)^9 - \frac{261857296733830119424}{47878893538482587890625}(x-x_n),$$

$$\gamma_0 = \frac{125(x-x_n)}{18144h^6}\left(\frac{2h}{5} - x + x_n\right)\left(-\frac{111088h^7}{78125} - \frac{55544h^6x}{15625} + \frac{55544h^6x_n}{15625} + \frac{161228h^5x^2}{3125} - \frac{322456h^5xx_n}{3125} + \frac{161228h^5x_n^2}{3125} - \frac{114686h^4x^2}{625} + \frac{344058h^4x^2x_n}{625} - \frac{344058h^4xx_n^2}{625} + \frac{114686h^4x_n^3}{625} + 328h^3x^4 - -1312h^3x^4 + 1968h^3x^2x_n^2 - 1312h^3xx_n^3 + 328h^3x_n^4 - \frac{1612h^2x^5}{5} + 1612h^2x^4x_n - 3224h^2x^3x_n^2 + 3224h^2x^2x_n^3 - 1612h^2xx_n^4 + \frac{1612h^2x_n^5}{5} + 166hx^6 - 996hx^5x_n + 2490hx^4x_n^2 - 3320hx^3x_n^3 + 2490hx^2x_n^4 - 996hxx_n^5 + 166hxx_n^6 - 35x^7 + 245x^6x_n - 735x^5x_n^2 + 1225x^4x_n^3 + 1225x^4x_n^3 - 1225x^3x_n^4 + 735x^2x_n^5 - 245xx_n^6 + 35x_n^7),$$

$$\gamma_{\frac{2}{5}} = \frac{1175(x-x_n)^5}{48h^2} - \frac{125(x-x_n)^4}{24h} - \frac{2675(x-x_n)^6}{54h^3} + \frac{625(x-x_n)^7}{12h^4} - \frac{3125(x-x_n)^8}{112h^5} + \frac{15625(x-x_n)^9}{2592h^6} + \frac{3002(x-x_n)}{70875},$$

$$\gamma_{\frac{3}{5}} = \frac{325(x-x_n)^5}{18h^2} - \frac{125(x-x_n)^4}{36h} - \frac{8675(x-x_n)^6}{216h^3} + \frac{23125(x-x_n)^7}{504h^4} - \frac{53125(x-x_n)^8}{2016h^5} + \frac{15625(x-x_n)^9}{2592h^6} + \frac{1598(x-x_n)}{70875},$$

$$\gamma_1 = \frac{7(x-x_n)^5}{15h^2} - \frac{(x-x_n)^4}{12h} - \frac{245(x-x_n)^6}{216h^3} + \frac{725(x-x_n)^7}{504h^4} - \frac{625(x-x_n)^8}{672h^5} + \frac{625(x-x_n)^9}{2592h^6} + \frac{842(x-x_n)}{1771875}.$$